Biochimica et Biophysica Acta 1813 (2011) 2157–2164

Contents lists available at ScienceDirect

Biochimica et Biophysica Acta

journal homepage: www.elsevier.com/locate/bbamcr

SK&F 96365 induces apoptosis and autophagy by inhibiting Akt–mTOR signaling in A7r5 cells

Eun-Jung Park [a,1], Sang-Yeob Kim [b,1], Su-Hwa Kim [a], Chae Ryun Lee [a], In-San Kim [b], Jong Kwan Park [c], Sung Won Lee [d], Byung Joo Kim [e], Jung Nyeo Chun [a,f], Insuk So [a,f], Ju-Hong Jeon [a,f,*]

[a] Department of Physiology, Seoul National University College of Medicine, Seoul 110-799, Republic of Korea
[b] Department of Biochemistry and Cell Biology, Cell and Matrix Research Institute, School of Medicine, Kyungpook National University, Daegu 700-422, Republic of Korea
[c] Department of Urology, Medical School, and Institute for Medical Sciences, Chonbuk National University, Jeonju 561-712, Republic of Korea
[d] Department of Urology, Samsung Medical Center, Sungkyunkwan University School of Medicine, Seoul 135-710, Republic of Korea
[e] School of Oriental Medicine, Pusan National University, Yangsan 626-770, Republic of Korea
[f] Institute of Dermatological Science, Medical Research Center Seoul National University, Seoul, Republic of Korea

ARTICLE INFO

Article history:
Received 15 February 2011
Received in revised form 20 June 2011
Accepted 21 June 2011
Available online 13 July 2011

Keywords:
SK&F 96365
Apoptosis
Autophagy
Akt–mTOR signaling
TRP channel

ABSTRACT

SK&F 96365 has been widely used as an inhibitor of transient receptor potential (TRP) calcium channels in various physiological settings. However, growing evidence suggests that SK&F 96365 affects several cellular and molecular processes via uncharacterized off-target mechanisms. In this study, we showed that SK&F 96365 induces apoptosis and autophagy in A7r5 vascular smooth muscle cells. The combined suppression of apoptosis and autophagy provoked necrosis rather than rescued cell death in the cells treated with SK&F 96365. In addition, we found that SK&F 96365 inhibits Akt–mTOR signaling pathways, which is comparable with the efficacy of other known Akt inhibitors. Our findings suggest that SK&F 96365 can be a useful agent for delineating the molecular mechanisms underlying crosstalk among cell death pathways.

1. Introduction

Vascular smooth muscle cells (VSMCs) play a crucial role in the regulation of blood vessel wall integrity and vascular tone. In pathological conditions, such as atherosclerosis and restenosis, VSMCs undergo phenotypic switching from a quiescent contractile to a proliferative synthetic phenotype [1,2]. Recent studies have shown that aberrant regulation of transient receptor potential (TRP) calcium channels underlies the pathogenesis of vascular proliferative diseases [3–5], suggesting that TRP channels can be promising targets for treatment of vascular proliferative diseases.

SK&F 96365, an imidazole derivative, has been widely used as a pharmacologic inhibitor of TRP channels (typically in the range of 10–100 μM) to assess the role of TRP channels in various pathophysiological processes [6,7]. However, growing evidence suggests that SK&F 96365 affects several cellular processes, including cell cycle arrest or cell death, in certain cells via uncharacterized off-target mechanisms [8–10]. Thus, the pharmacologic effects of SK&F 96365 need to be carefully evaluated to avoid misinterpretation of the data. Nonetheless, little has been known about the mechanisms underlying off-target effects of SK&F 96365.

Apoptosis and autophagy are self-destructive processes that play a crucial role in the pathophysiological remodeling of injured tissues [11,12]. Deregulation of these processes is associated with various human diseases, including vascular proliferative diseases and cancers [13]. Apoptosis and autophagy share many common molecular regulators or pathways [12,14]. For example, Akt, mTOR or Bcl-2 inhibits both apoptosis and autophagy [14], whereas BNIP3 induces both processes [12]. However, the relationship between apoptosis and autophagy is very complex: they are synergistic or antagonistic to each other to induce cell death in a cell type- and/or context-specific manner [12]. Moreover, under certain conditions, the concurrent inhibition of apoptosis and autophagy can lead to necrotic cell death [15,16]. Therefore, the better understanding of crosstalk among cell death pathways may be a key to develop therapeutic strategies to improve the efficacy of the drugs targeting proliferative diseases, including restenosis and cancers.

As an attempt to understand the off-target action of SK&F 96365, we have investigated the mechanisms underlying cell death induced by SK&F 96365. In this study, we showed that SK&F 96365 induces both

Abbreviations: TRP channel, transient receptor potential channel; VSMC, vascular smooth muscle cell; 3-MA, 3-methyladenine

* Corresponding author at: Department of Physiology, Seoul National University College of Medicine, 28 Yongon-Dong, Chongno-Gu, Seoul 110-799, Republic of Korea. Tel.: +82 2 740 8399; fax: +82 2 763 9667.
E-mail address: jhjeon2@snu.ac.kr (J.-H. Jeon).

[1] These authors contributed equally to this work.

0167-4889/$ – see front matter © 2011 Published by Elsevier B.V.
doi:10.1016/j.bbamcr.2011.06.021

apoptosis and autophagy in A7r5, a VSMC line, via off-target mechanism (s). We found that SK&F 96365 has the ability to inhibit Akt–mTOR signaling pathways with similar IC_{50} values of other known Akt inhibitors. Our findings suggest that SK&F 96365 is applicable as a novel Akt-targeting agent for the treatment of proliferative diseases.

2. Materials and methods

2.1. Cell culture and reagents

A7r5 cells were purchased from ATCC. The cells were cultured in DMEM supplemented with 10% fetal bovine serum, penicillin (100 U/ml), and streptomycin (100 μg/ml). All cell culture agents used were obtained from Hyclone or Invitrogen. SK&F 96365, LOE 908, Pyr2, and Pyr3 were purchased from Tocris. All other reagents not specified were supplied by Sigma.

2.2. Cell viability assay

A7r5 cells were grown in 12-well culture plates. MTT or LDH release assay was used to assess cell viability according to the manufacturers' instructions (Sigma or Promega). The assays were quantitated by measuring the absorbance at 570 or 490 nm on microplate spectrophotometer (ASYS).

2.3. Flow cytometry analysis

A7r5 cells were fixed with 70% ethanol and then labeled with propidium iodide solution (50 μg/ml) containing RNase A (100 μg/ml). The percentage of sub-G1 cells was obtained by cell cycle profile analysis using flow cytometry (BD Biosciences). ModFitLT V3.0 software was used for data analysis.

2.4. Caspase assay

The activity of caspase-3 and -9 from A7r5 cells was determined in microtiter plates as previously described [17]. Ac-DEVD-P-nitroaniline and Ac-LEHD-P-nitroaniline (AG scientific) at 2 mM were used for caspase-3 and -9 assays, respectively. P-nitroaniline was used to generate the standard curve to evaluate the concentration of the products. A pan-caspase inhibitor zVAD-fmk (Calbiochem) was used to validate the assay method. The absorbance was measured at 405 nm on microplate spectrophotometer (ASYS).

2.5. Assessment of mitochondrial membrane depolarization

Mitochondrial membrane depolarization was evaluated using JC-1 fluorescence probe according to the manufacturer's instructions (Molecular Probes). A7r5 cells were labeled with 2 μM JC-1 for 30 min at 37 °C and then analyzed by flow cytometry using 488 nm excitation with 530/30 or 585/42 nm bypass emission filters. The cells without red

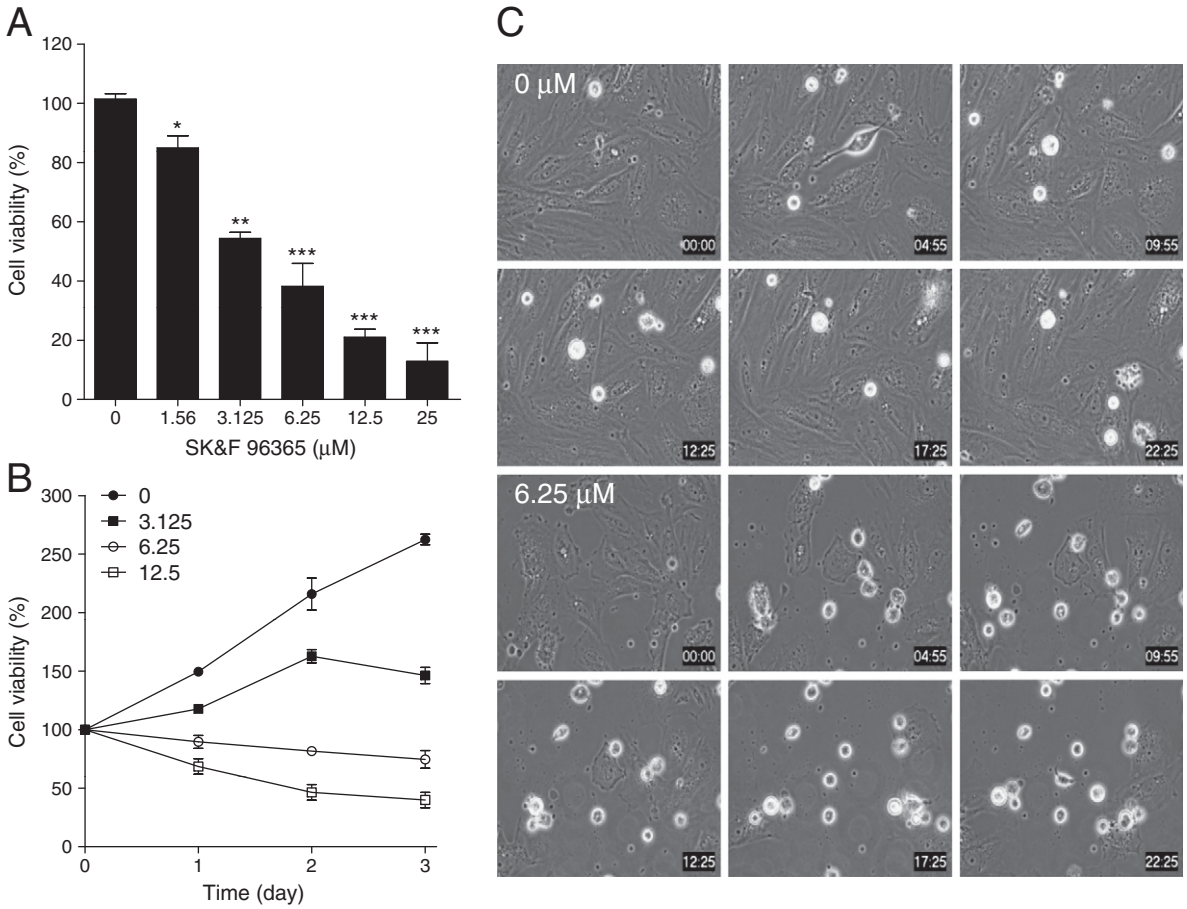

Fig. 1. SK&F 96365 induces cell death in A7r5 cells. (A) The cells were incubated with SK&F 96365 at the indicated concentrations for 72 h prior to MTT assays. Distilled water was used as vehicle. Cell viability is expressed as a relative value to that of the untreated cells which is set to 100%. The figures show mean ± SEM (n = 4). $^{*}P<0.05$, $^{**}P<0.01$, $^{***}P<0.005$. (B) Time course response to SK&F 96365. Cell viability is expressed as a relative value to that of the cells treated with vehicle and harvested at zero time which is set to 100%. (C) Time-lapse image of A7r5 cells treated with SK&F 96365. Of the images obtained every 1 min for 24 h, the selected images were shown.

fluorescence were regarded as the cells manifesting mitochondrial membrane depolarization.

2.6. Intracellular Ca^{2+} measurement

The detached A7r5 cells were incubated with 5 μM Fura-2-AM and 0.02% Pluronic F-127 (Molecular probes) in normal Tyrode's solution (10 mM HEPES, 145 mM NaCl, 3.6 mM KCl, 1 mM $MgCl_2$, 1.3 mM $CaCl_2$, and 5 mM glucose) for 50 min at 37 °C. After washing twice, the cells were resuspended with normal Tyrode's solution. Fluorescence emission at 510 nm was measured with excitation at 340/380 nm in a stirred quartz-microcuvette of fluorescence spectrophotometer (Photon Technology Instrument). Maximum and minimum fluorescence values at 380 nm (F_{max} and F_{min}) were calibrated by addition of 0.2% Triton X-100 and 10 mM EGTA, respectively. The $[Ca^{2+}]_{cyt}$ was calculated from the equation, $[Ca^{2+}] = Kd \times \beta \times (R - R_{min})/(R_{max} - R)$ where Kd is the dissociation constant for Fura-2 (224 nM), β is F_{min}/F_{max}, and R is F340/F380.

2.7. Quantitative analysis of GFP-LC3 dot

A7r5 cells were transfected with GFP-LC3 using Fugene-6 (Roche). The cells expressing GFP-LC3 were directly observed by FluoView 1000 confocal microscopy (Olympus). The number of GFP-LC3 dots in each cell (total 40–50 cells) was counted in at least five independent visual fields.

2.8. Western blot analysis

The crude extracts from A7r5 cells were prepared by incubation with RIPA buffer containing protease and phosphatase inhibitor cocktails (Calbiochem). The proteins were resolved in 6, 10, or 15% SDS–PAGE and analyzed with the antibodies indicated. Antibodies to cleaved caspase-3, Akt, $pAkt^{S473}$, $pGSK3\beta^{S9}$, mTOR, $pmTOR^{S2448}$, Mcl-1, Beclin-1, and BINP3 were purchased from Cell Signaling. Antibody to LC-3 was obtained from Medical and Biological Laboratories. Antibodies to Bcl-2, GSK3β, Bax, and GAPDH were supplied by Santa Cruz. Antibody to PARP was obtained from BD Pharmingen.

2.9. Live cell imaging

A7r5 cells were plated onto a collagen-coated 35-mm glass-base dish (Asahi techno glass) and grown overnight at 37 °C. To obtain phase contrast images, the cells were placed in an incubation chamber equipped with a time-lapse imaging system (Nikon BioStation IM). The images were captured at 5 min intervals. To perform time-lapse image analysis for autophagy, the cells transfected with GFP-LC3 were imaged with a Leica DM IRB inverted microscope (Leica Microsystems) equipped with Cascade 512B (EMCCD) camera (Roper Scientific). All images were processed using MetaMorph software (Universal Imaging).

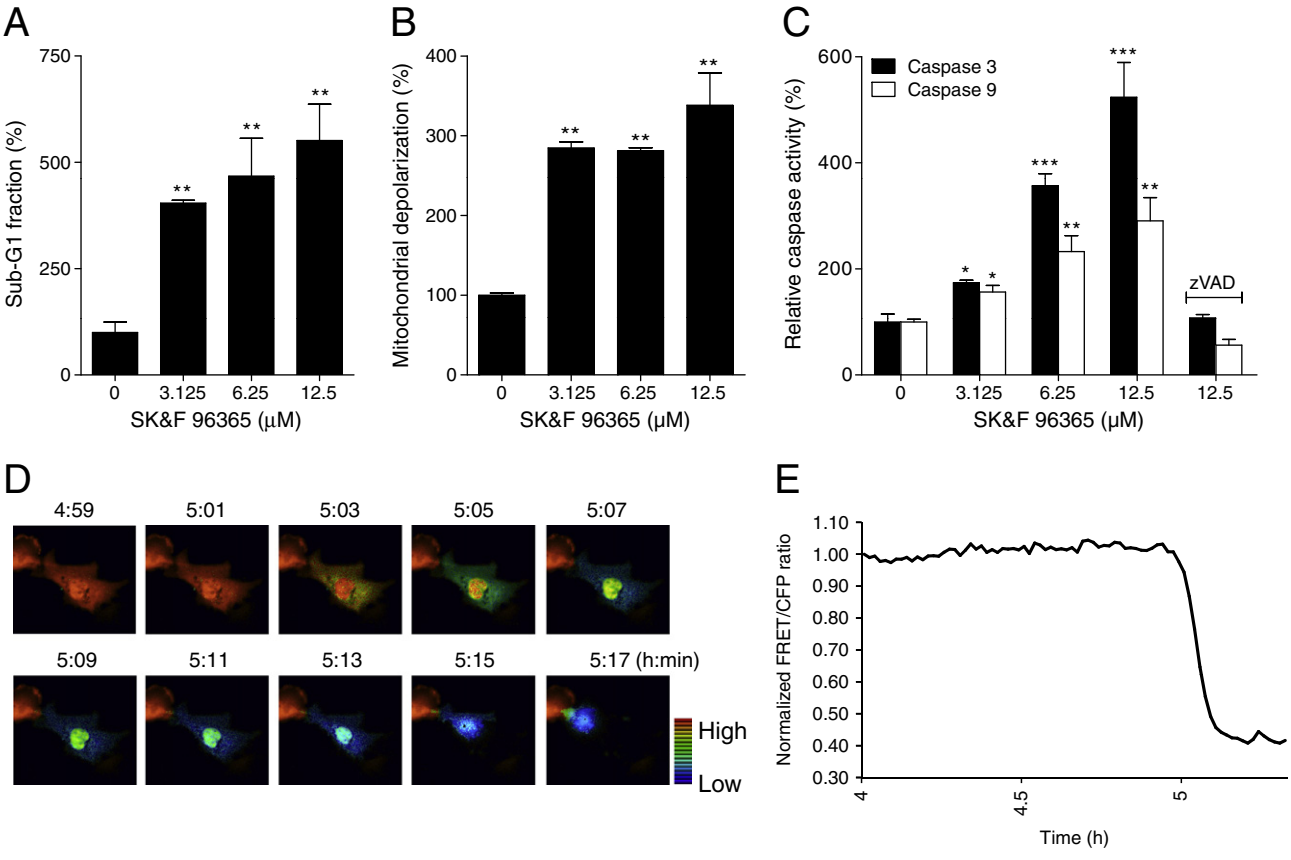

Fig. 2. SK&F 96365 triggers apoptosis in A7r5 cells. The cells were cultured with SK&F 96365 at the indicated concentrations for 24 h prior to labeling with propidium iodide (A) or JC-1 dye (B). (A) Cell fraction is expressed as the percentage of sub-G1 cells. (B) Mitochondria membrane depolarization is expressed as a relative value to that of untreated cells which is set to 100%. (C) The cells were cultured with SK&F 96365 at the indicated concentrations for 24 h prior to caspase assays. Caspase activity from untreated cells is expressed as 100%. Pan-caspase inhibitor zVAD-fmk (zVAD) at 20 μM was used to validate the analytical method employed. (D) Caspase-3 activity was monitored by SCAT3 FRET-based indicator in A7r5 cells treated with SK&F 96365 at 6.25 μM. CFP (excitation 440 nm/emission 480 nm) and FRET (excitation 440 nm/emission 530 nm) images were obtained every 1 min with a time-laps epifluorescecnt microscope. The ratio images of FRET/CFP were prepared by using MetaMorph software and the representative images were presented. (E) FRET/CFP emission ratio changes of the SK&F 96365-treated cells. The emission ratio values were normalized to those of the record-starting time. The figures show mean ± SEM (n = 4–6). $^{*}P<0.05$, $^{**}P<0.01$, $^{***}P<0.005$.

2.10. FRET imaging

A7r5 cells were cultured on a collagen-coated 35-mm glass-base dish and transfected with caspase-3 FRET-based indicator (SCAT3) as previously described [18]. FRET images were captured by a Leica DM IRB inverted microscope equipped with Cascade 512B (EMCCD) camera, excitation and emission filter wheels (MAC5000, Ludl Electronic Products). All systems were controlled by MetaMorph software. The fluorescent images were sequentially obtained through CFP and FRET filter channels. Filter sets and ND filters were purchased from Chroma Technology (Rockingham). The images were obtained by using the 2×2 or 3×3 binning mode and 100-ms exposure time. The ratio image of FRET/CFP was created with MetaMorph software.

2.11. Statistic analysis

All data are expressed as mean ± SEM. Comparison of means among experimental groups was carried out with ANOVA followed by a post hoc test. $P<0.05$ was considered statistically significant.

3. Results

3.1. SK&F 96365 induces cell death in A7r5 cells

To ascertain whether SK&F 96365 kills A7r5 cells, we performed MTT assays. Viable cell population was gradually reduced in relation to concentrations of SK&F 96365 with the IC_{50} value of 3.18 μM (Fig. 1A), which was verified by quantitating cell growth over time (Fig. 1B). To confirm MTT assay results further, we monitored SK&F 96365-induced cell death by a time-lapse imaging system. The cells were detached upon SK&F 96365 over times compared to vehicle (Fig. 1C). Thus, our results demonstrate that SK&F 96365 induces cell death in A7r5 cells.

3.2. SK&F 96365 triggers apoptosis in A7r5 cells

To determine whether SK&F 96365 induces cell death by apoptosis, we first analyzed cell cycle profiles. Flow cytometric analysis showed that the percentage of sub-G1 phase cells markedly increases in the cells treated with SK&F 96365 in a dose-dependent manner (Fig. 2A). In addition, SK&F 96365 elevated mitochondrial membrane depolarization, an early event of an intrinsic apoptosis signaling (Fig. 2B). Thus, our findings suggest that SK&F 96365 induces apoptosis via intrinsic apoptotic mechanism(s).

To corroborate our observations, we performed caspase activity assays. SK&F 96365 increased the activity of caspase-3 and -9, which was restrained by zVAD-fmk, a pan-caspase inhibitor (Fig. 2C). These results were further confirmed by time-lapse image analysis using caspase-3 FRET-based indicator (SCAT3). A decrease in FRET signals was observed after 5 h of treatment with SK&F 96365, which means that SK&F 96365 activates caspase-3 (Fig. 2D and E). In addition, Western blot analysis showed that SK&F 96365 produces cleaved caspase-3, an

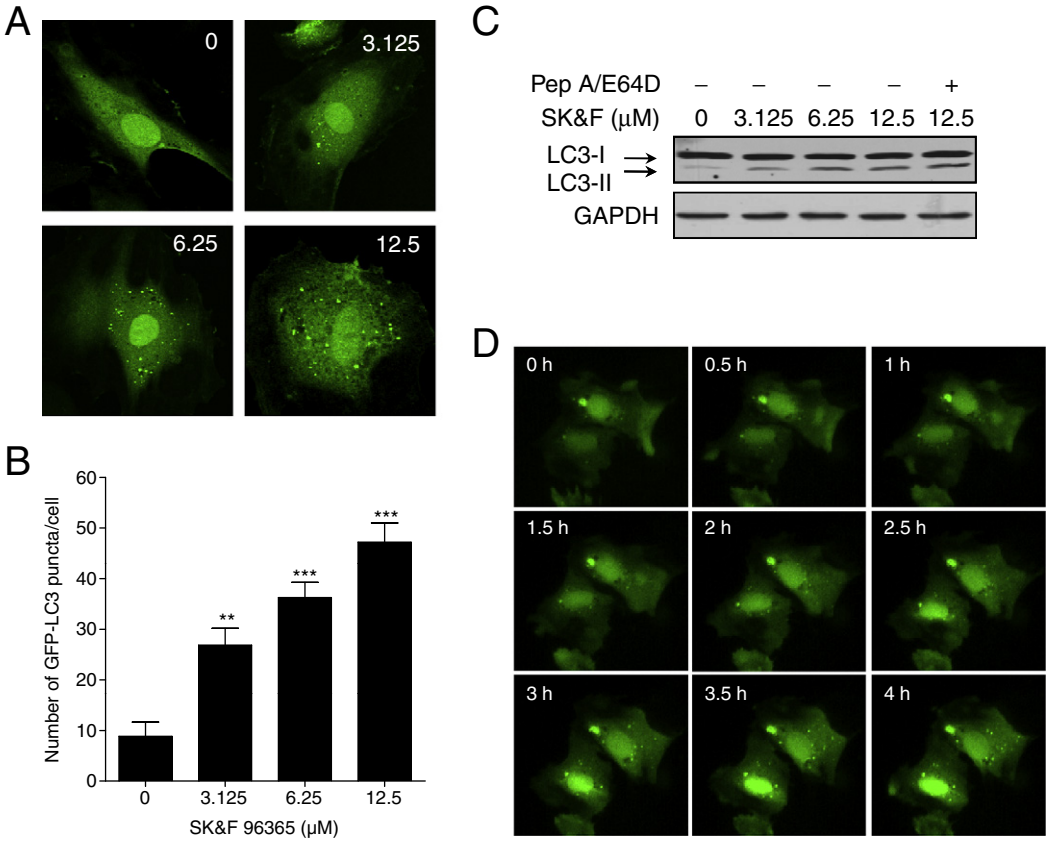

Fig. 3. SK&F 96365 induces autophagy in A7r5 cells. (A) A7r5 cells expressing GFP-LC3 were directly observed by confocal microscopy following treatment with SK&F 96365 for 24 h. (B) The number of GFP-LC3 dots in each cell was counted in at least five independent visual fields. The figure shows mean ± SEM (n = 40–50). $^{**}P<0.01$, $^{***}P<0.005$. (C) LC3 was assessed by western blot analysis using the crude extract prepared from the cells treated with SK&F 96365 for 24 h. Pepstatin A and E64D (Pep A/E64D) at 10 μM each, lycosomal protease inhibitors, were included to corroborate LC3-II production. Western blots are representative of three independent experiments. (D) Dynamics of autophagosome formation in live cells following treatment with SK&F 96365. Live-cell imaging was performed on A7r5 cells expressing GFP-LC3 in the presence of 6.25 μM SK&F 96365. The images were acquired every 1 min with a time-laps epifluorescecnt microscope and the representative images were presented.

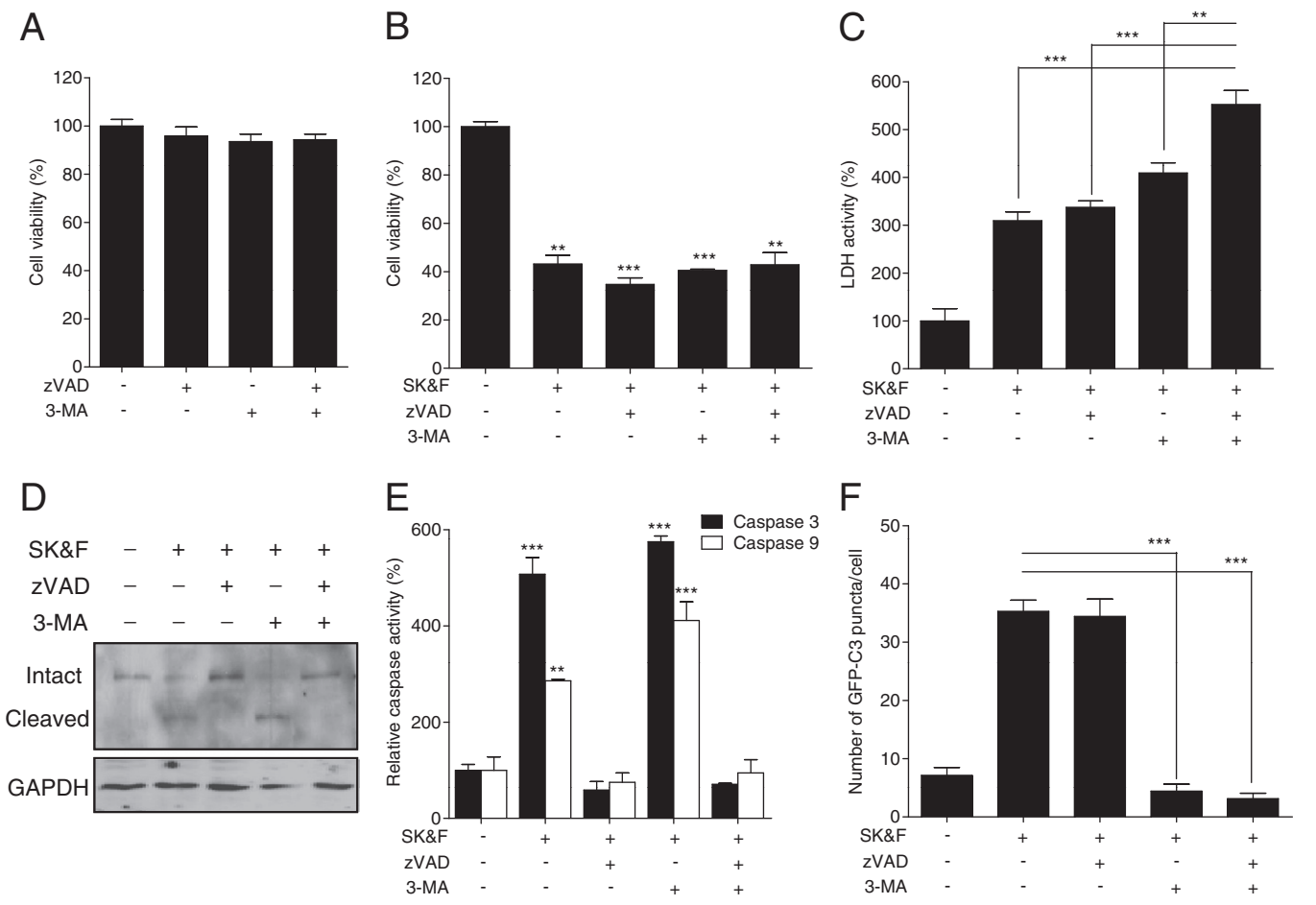

Fig. 4. The combined suppression of apoptosis and autophagy promotes necrosis in A7r5 cells. The used concentrations of SK&F 96365, zVAD-fmk, and 3-MA were 6.25 μM, 20 μM, and 1 mM, respectively. The cells were treated with zVAD-fmk and/or 3-MA for 72 h in the absence (A) or presence (B) of SK&F 96365. Cell viability is expressed as a relative value to that of the untreated cells which is set to 100%. The figure shows mean ± SEM (n = 4). (C) The cells were cultured with SK&F 96365, zVAD-fmk, and/or 3-MA for 48 h prior to LDH assays. LDH activity is expressed as a relative value to that of the untreated cells which is set to 100%. The figure shows mean ± SEM (n = 4). (D) PARP cleavage was assessed by western blot analysis using the crude extract prepared from the cells treated with SK&F 96365, zVAD-fmk and/or 3-MA for 24 h. Western blots are representative of three independent experiments. (E) The cells were cultured with SK&F 96365, zVAD-fmk and/or 3-MA for 24 h prior to caspase assays. Caspase activity from untreated cells is expressed as 100%. (F) The cells were cultured with SK&F 96365, zVAD-fmk and/or 3-MA for 24 h prior to confocal image analysis. The number of GFP-LC3 dots in each cell was counted in at least five independent visual fields. The figure shows mean ± SEM (n = 40–50). $^{**}P<0.01$, $^{***}P<0.005$.

enzymatically active form (SFig. 1). Furthermore, SK&F 96365 reduced the expression of pro-survival Bcl-2 and Mcl-1, whereas it elevated that of anti-survival Bax, Beclin-1, and BNIP3 (SFig. 1). These results demonstrate that SK&F 96365 triggers apoptosis. Nonetheless, zVAD-fmk failed to rescue cell death (SFig. 2), suggesting that apoptosis is not the sole mechanism for SK&F 96365-induced cell death.

3.3. SK&F 96365 induces autophagy in A7r5 cells

We then questioned whether SK&F 96365 induces cell death via autophagy. Fluorescence image analysis showed that distinct GFP-LC3 dots, an autophagy marker, appear in the cells treated with SK&F 96365 (Fig. 3A). When GFP-LC3 dots were counted in each cell (total 40–50 cells), the number of dots gradually increased in relation to concentrations of SK&F 96365 (Fig. 3B). Western blot analysis revealed that SK&F 96365 increases the level of LC3-II, a biomarker of autophagy (Fig. 3C). In addition, time-lapse microscopic analysis showed that an increase in GFP-LC3 dots appears after 2 h of treatment with SK&F 96365 (Fig. 3D). These results demonstrate that SK&F 96365 induces both apoptosis and autophagy.

To assess the specificity of SK&F 96365 action, we examined the effects of other TRP channel blockers, which include LOE 908 [21], Pyr2, Pyr3 [22,23], and 2APB [24], on apoptosis and autophagy. MTT assays showed that the cytotoxic activities of TRP channel blockers are different from each other (SFig. 3A–D). We then evaluated apoptosis in terms of caspase activity using the blockers at the typically used concentrations (10 μM LOE 908, 10 μM Pyr2, 10 μM Pyr3, and 100 μM 2APB). Among these blockers, only 2APB was able to induce apoptosis (SFig. 3E). However, GFP-LC3 puncta analysis showed that all four blockers do not trigger autophagy (SFig. 3F). These results indicate that SK&F 96365 specifically induces both apoptosis and autophagy, probably via a TRP channel-independent manner.

3.4. Suppression of apoptosis and autophagy promotes necrotic cell death in A7r5 cells

Because several papers have reported that the combined suppression of apoptosis and autophagy enables necrosis [15,16], we questioned the phenotypic consequence of concurrent suppression of apoptosis and autophagy in the cells treated with SK&F 96365. We first ascertained that zVAD-fmk and/or 3-methyladenine (3-MA), a type III PI3K inhibitor, does not affect cell viability (Fig. 4A). However, SK&F 96365-induced cell death was not rescued by the combined treatment of zVAD-fmk and 3-MA (Fig. 4B). We thus assessed necrotic cell death using LDH release assays (Fig. 4C). SK&F 96365 caused 3-fold increase in LDH activity. Under these conditions, neither zVAD-fmk nor 3-MA suppressed the elevated LDH activity. On the contrary, co-treatment of zVAD-fmk and 3-MA resulted in 5.5-fold increase in

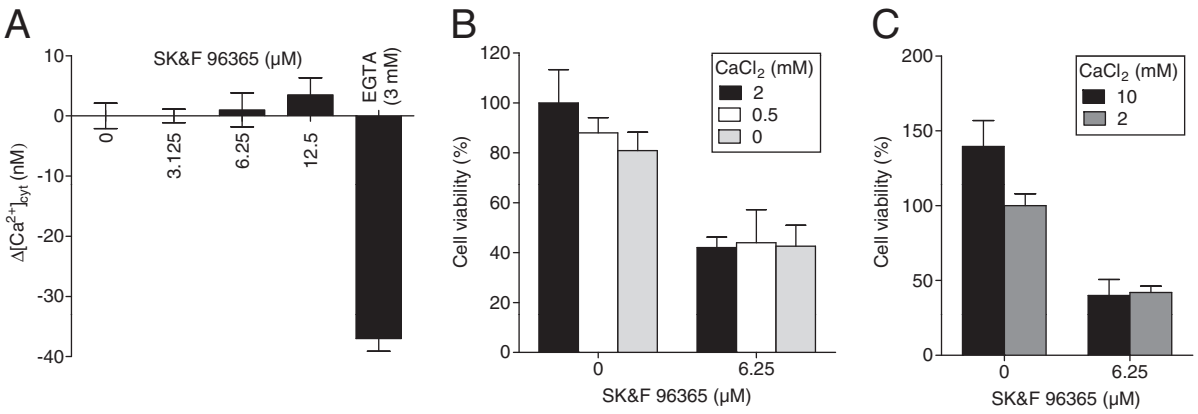

Fig. 5. SK&F 96365 cytotoxicity is unrelated to intracellular or extracellular calcium concentrations in A7r5 cells. (A) The $[Ca^{2+}]_{cyt}$ was measured using Fura-2 in the absence of presence of SK&F 96365 (SK&F). EDTA at 3 mM was used to validate the analytical method employed. (B–C) MTT assays were performed following treatment with SK&F 96365 for 48 h. Extracellular $[Ca^{2+}]$ was adjusted by addition of $CaCl_2$ solution to Ca^{2+}-free DMEM. The Ca^{2+} included in 10% FBS was not removed in the experiments. The figure shows mean ± SEM (n = 4).

LDH activity. These results indicate that the combined inhibition of apoptosis and autophagy provokes necrosis in the cells treated with SK&F 96365.

To verify the functionality of zVAD-fmk and 3-MA, we first examined the cleavage of PARP, a caspase-3 substrate. SK&F 96365 produced a cleaved form of PARP, which is blocked by zVAD-fmk, but not 3-MA (Fig. 4D). These results well correlated with those from caspase activity assays (Fig. 4E). We also measured the number of GFP-LC3 puncta. 3-MA suppressed GFP-LC3 puncta formation in SK&F 96365-treated cells, whereas zVAD-fmk did not affect it (Fig. 4F and SFig. 4). These results showed that zVAD-fmk and 3-MA specifically inhibit apoptosis and autophagy, respectively.

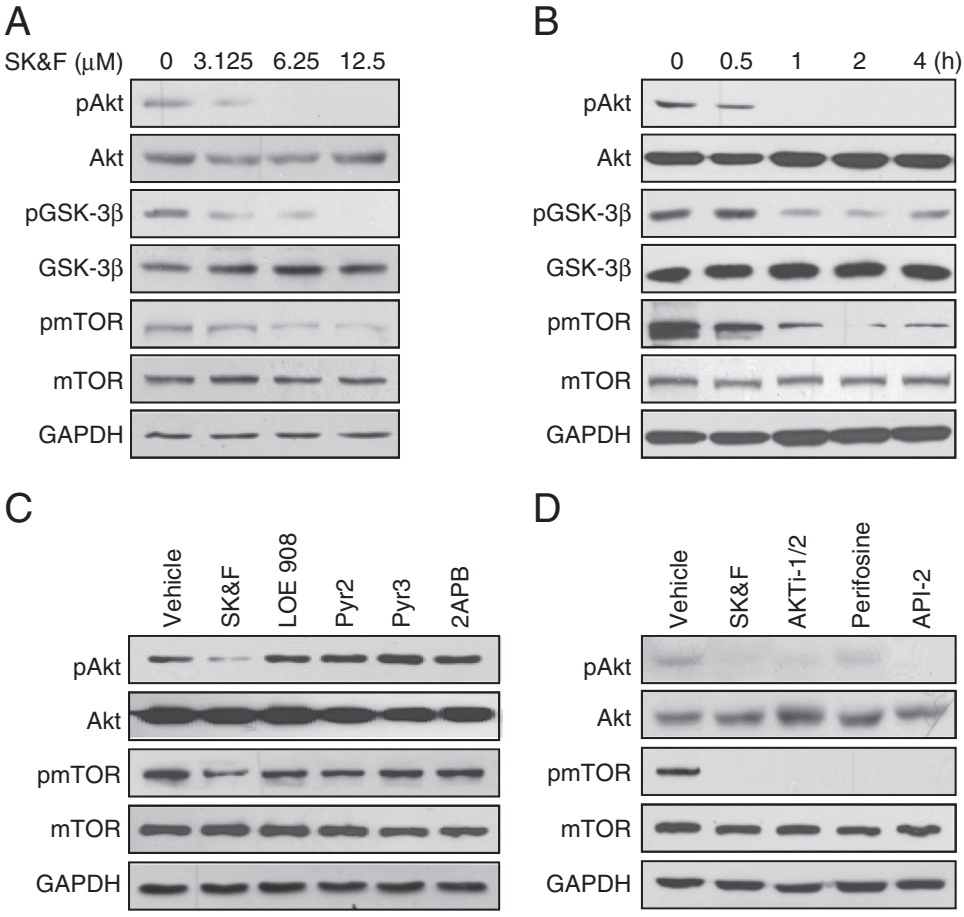

Fig. 6. SK&F 96365 inhibits Akt–mTOR signaling in A7r5 cells. Western blot analysis was performed using the crude extracts that were prepared from the cells treated with SK&F 96365 at the indicated concentrations for 4 h (A) or at 6.25 μM for the indicated times (B). (C) SK&F 96365 (6.25 μM), LOE 908 (10 μM), Pyr2 (10 μM), Pyr3 (10 μM), or 2APB (100 μM) were treated for 4 h. (D) SK&F 96365 (3.18 μM), AKTi-1/2 (2.51 μM), perifosine (5.04 μM), and API-2 (2.7 μM) were treated for 4 h. Western blots are representative of 3–4 independent experiments.

3.5. SK&F 96365 cytotoxicity is unrelated to intracellular or extracellular calcium concentrations in A7r5 cells

To get a clue to the mechanisms of SK&F 96365-induced cell death, we examined the effect of SK&F 96365 on cytoplasmic calcium concentration ($[Ca^{2+}]_{cyt}$). As shown in Fig. 5A, SK&F 96365 did not affect $[Ca^{2+}]_{cyt}$, whereas EGTA significantly reduced $[Ca^{2+}]_{cyt}$. We then measured the changes in cell viability depending on different extracellular calcium concentrations ($[Ca^{2+}]_{ext}$). Lowering $[Ca^{2+}]_{ext}$ did not accelerate SK&F 96365-induced cell death (Fig. 5B). In addition, elevated $[Ca^{2+}]_{ext}$ failed to rescue the cell death (Fig. 5C). These results indicate that SK&F 96365 induces cell death via the mechanisms independent of intracellular or extracellular calcium concentrations.

To evaluate the effect of SK&F 96365 on TRP channel activity, particularly TRPM7 and TRPC5 in this study, we performed whole-cell patch clamp analysis. SK&F 96365 at 6.25 μM (SFig. 5) or 12.5 μM (data not shown) did not affect the currents of TRPM7 (SFig. 5A–C) and TRPC5 (SFig. 5D–F). By contrast, SK&F 96365 at 100 μM inhibited the currents of these TRP channels, suggesting that more than a dozen concentrations of SK&F 96365 are effective in inhibiting TRP channel activity. It is worthwhile to note that SK&F 96365 at 6.25 μM is able to influence on the calcium mobilization pattern induced by AVP (SFig. 6A), whereas SK&F 96365 at 3.125 μM does not affect it (SFig. 6B). Because 3.125 μM of SK&F 96365 is sufficient to induce apoptosis and autophagy (Figs. 1–3), our data suggest that the action of SK&F 96365 may be unrelated to calcium transport pathways.

3.6. SK&F 96365 inhibits Akt–mTOR signaling pathways in A7r5 cells

To understand the molecular actions of SK&F 96365, we performed Western blot analysis with A7r5 cells. Because Akt–mTOR signaling pathways antagonize both apoptosis and autophagy [12,14], we first assessed whether SK&F 96365 inhibits Akt–mTOR signaling. SK&F 96365 decreased the phosphorylation level of Akt at Ser-473, an indicator of Akt activity, in a concentration-dependent manner (Fig. 6A). These results were comparable with the phosphorylation level of GSK-3β (an Akt substrate) and mTOR (an Akt effector). The inhibition of Akt–mTOR signaling was observed following treatment with SK&F 96365 for 30 min and sustained thereafter (Fig. 6B). Moreover, the inhibitory action on Akt–mTOR signaling was specific for SK&F 96365 and other TRP channel blockers did not inhibit Akt–mTOR signaling (Fig. 6C).

To assess the usefulness of SK&F 96365 as a novel inhibitor of Akt–mTOR signaling, we compared the cytotoxic efficacy of SK&F 96365 with other known Akt inhibitors that have been developed as anticancer agents. The IC_{50} values obtained from MTT assays were approximately 3.18, 2.51, 5.04, and 2.7 μM for SK&F 96365, AKTi-1/2, perifosine, and API-2, respectively (data not shown). At these concentrations, all chemicals obviously inhibited Akt–mTOR signaling (Fig. 6D).

4. Discussion

In this study, we demonstrate that SK&F 96365 induces apoptosis and autophagy in A7r5 cells. Under the conditions, the concurrent suppression of apoptosis and autophagy was found to causes necrotic cell death. The cytotoxic activity of SK&F 96365 was unrelated to calcium transport pathways. We also showed that SK&F 96365 inhibits Akt–mTOR signaling, which can underlie an important mechanism of SK&F 96365-induced cell death.

The interaction between apoptosis and autophagy is exceptionally complex and the underlying molecular mechanisms are poorly understood [12]. Our data propose that SK&F 96365 is a useful chemical probe to assess the crosstalk among cell death processes on the molecular level. Thus, chemical biology with SK&F 96365 will assist in discovering the molecular interactions governing relationship among apoptosis, autophagy, and necrosis. In addition, we found that SK&F 96365 modulates Akt–mTOR signaling and Bcl-2 family expression, which provides insight into the future research aimed to illuminate the molecular mechanisms of SK&F 96365 actions.

Many Akt and mTOR inhibitors have been developed to treat proliferation-related diseases, including restenosis and cancers [19]. Particularly, the loss-of-function mutations in PTEN leading to Akt–mTOR activation are frequently observed in several types of cancers [20]. We showed that the efficacy of SK&F 96365 is comparable with other Akt inhibitors, such as perifosine, Akti-1/2, and API-2. In our preliminary study, we found that SK&F 96365 suppresses the cell growth of PC-3 (IC_{50} = 3.28 μM) and LNCaP (IC_{50} = 1.52 μM), PTEN-negative prostate cancer cell lines (data not shown). Therefore, these data suggest that SK&F 96365 can be a promising anticancer agent inhibiting Akt–mTOR signaling.

SK&F 96365 has been widely used to delineate the causal role of TRP channels in the pathophysiological processes of cardiovascular or nerve systems, typically in the range of 10–100 μM [6,7]. Of the TRP channel blockers used, SK&F 96365 was found to have a potent cytotoxic activity and inhibit Akt–mTOR signaling, suggesting that the actions of SK&F 96365 are unrelated to TRP channel inhibition. However, several questions still remain to be determined. Firstly, it is needed to investigate whether SK&F 96365 at 6.25 μM can affect the currents of other TRP channels rather than TRPM7 and TRPC5. Secondly, most TRP channels are not exclusive to calcium and in fact permeable to potassium, sodium, magnesium, and proton. In this study, we did not address an issue concerning ion permeability or selectivity. Thirdly, there is a possibility that TRP channels are inhibited by SK&F 96365 via the Akt–mTOR signaling pathways. Nonetheless, our results show that the treatment time and dosage of SK&F 96365 should be carefully optimized to exclude its off-target effects. In addition, our findings suggest that cautious interpretation is required when SK&F 96365 is included in the assay systems.

In summary, our results demonstrated that SK&F 96365 induces both apoptosis and autophagy in A7r5 cells. In addition, we showed that SK&F 96365 is a novel inhibitor of Akt–mTOR signaling pathways. Thus, our findings suggest that SK&F 96365 is a useful chemical probe to assist in understanding cell death processes and their related diseases.

Acknowledgement

A plasmid for caspase-3 FRET-based indicator (SCAT3) was kindly provided by Prof. Takeharu Nagai from Hokkaido University in Japan. This study was supported by a grant of the Korea Health 21R&D project, Ministry of Health, Welfare and Family Affairs, Republic of Korea (A090583).

Appendix A. Supplementary data

Supplementary data to this article can be found online at doi:10.1016/j.bbamcr.2011.06.021.

References

[1] G.K. Owens, M.S. Kumar, B.R. Wamhoff, Molecular regulation of vascular smooth muscle cell differentiation in development and disease, Physiol. Rev. 84 (2004) 767–801.
[2] V.J. Dzau, R.C. Braun-Dullaeus, D.G. Sedding, Vascular proliferation and atherosclerosis: new perspectives and therapeutic strategies, Nat. Med. 8 (2002) 1249–1256.
[3] J. Soboloff, M. Spassova, W. Xu, L.P. He, N. Cuesta, D.L. Gill, Role of endogenous TRPC6 channels in Ca^{2+} signal generation in A7r5 smooth muscle cells, J. Biol. Chem. 280 (2005) 39786–39794.
[4] C.S. Facemire, P.J. Mohler, W.J. Arendshorst, Expression and relative abundance of short transient receptor potential channels in the rat renal microcirculation, Am. J. Physiol. Renal Physiol. 286 (2004) F546-F551.

[5] D.E. Clapham, L.W. Runnels, C. Strubing, The TRP ion channel family, Nat. Rev. Neurosci. 2 (2001) 387–396.
[6] X. Zhu, M. Jiang, L. Birnbaumer, Receptor-activated Ca^{2+} influx via human Trp3 stably expressed in human embryonic kidney (HEK)293 cells. Evidence for a non-capacitative Ca^{2+} entry, J. Biol. Chem. 273 (1998) 133–142.
[7] F. Pena, B. Ordaz, Non-selective cation channel blockers: potential use in nervous system basic research and therapeutics, Mini Rev. Med. Chem. 8 (2008) 812–819.
[8] L. Zhang, J. Yu, H. Pan, P. Hu, Y. Hao, W. Cai, H. Zhu, A.D. Yu, X. Xie, D. Ma, J. Yuan, Small molecule regulators of autophagy identified by an image-based high-throughput screen, Proc. Natl. Acad. Sci. U.S.A. 104 (2007) 19023–19028.
[9] T. Nordstrom, H.A. Nevanlinna, L.C. Andersson, Mitosis-arresting effect of the calcium channel inhibitor SK&F 96365 on human leukemia cells, Exp. Cell Res. 202 (1992) 487–494.
[10] Y. Kawanabe, N. Hashimoto, T. Masaki, Ca(2+) channels involved in endothelin-induced mitogenic response in carotid artery vascular smooth muscle cells, Am. J. Physiol. Cell Physiol. 282 (2002) C330-C337.
[11] A. Degterev, J. Yuan, Expansion and evolution of cell death programmes, Nat. Rev. Mol. Cell Biol. 9 (2008) 378–390.
[12] M.C. Maiuri, E. Zalckvar, A. Kimchi, G. Kroemer, Self-eating and self-killing: crosstalk between autophagy and apoptosis, Nat. Rev. Mol. Cell Biol. 8 (2007) 741–752.
[13] R.S. Hotchkiss, A. Strasser, J.E. McDunn, P.E. Swanson, Cell death, N. Engl. J. Med. 361 (2009) 1570–1583.
[14] A. Eisenberg-Lerner, S. Bialik, H.U. Simon, A. Kimchi, Life and death partners: apoptosis, autophagy and the cross-talk between them, Cell Death Differ. 16 (2009) 966–975.
[15] E. White, Autophagic cell death unraveled: pharmacological inhibition of apoptosis and autophagy enables necrosis, Autophagy 4 (2008) 399–401.
[16] K. Kunchithapautham, B. Rohrer, Apoptosis and autophagy in photoreceptors exposed to oxidative stress, Autophagy 3 (2007) 433–441.
[17] G.Y. Jang, J.H. Jeon, S.Y. Cho, D.M. Shin, C.W. Kim, E.M. Jeong, H.C. Bae, T.W. Kim, S.H. Lee, Y. Choi, D.S. Lee, S.C. Park, I.G. Kim, Transglutaminase 2 suppresses apoptosis by modulating caspase 3 and NF-kappaB activity in hypoxic tumor cells, Oncogene 29 (2010) 356–367.
[18] K. Takemoto, T. Nagai, A. Miyawaki, M. Miura, Spatio-temporal activation of caspase revealed by indicator that is insensitive to environmental effects, J. Cell Biol. 160 (2003) 235–243.
[19] T.A. Yap, M.D. Garrett, M.I. Walton, F. Raynaud, J.S. de Bono, P. Workman, Targeting the PI3K–AKT–mTOR pathway: progress, pitfalls, and promises, Curr. Opin. Pharmacol. 8 (2008) 393–412.
[20] J. Li, C. Yen, D. Liaw, K. Podsypanina, S. Bose, S.I. Wang, J. Puc, C. Miliaresis, L. Rodgers, R. McCombie, S.H. Bigner, B.C. Giovanella, M. Ittmann, B. Tycko, H. Hibshoosh, M.H. Wigler, R. Parsons, PTEN, a putative protein tyrosine phosphatase gene mutated in human brain, breast, and prostate cancer, Science 275 (1997) 1943–1947.
[21] D. Wicher, H.J. Agricola, R. Schonherr, S.H. Heinemann, C. Derst, TRPgamma channels are inhibited by cAMP and contribute to pacemaking in neurosecretory insect neurons, J. Biol. Chem. 281 (2006) 3227–3236.
[22] S. Kiyonaka, K. Kato, M. Nishida, K. Mio, T. Numaga, Y. Sawaguchi, T. Yoshida, M. Wakamori, E. Mori, T. Numata, M. Ishii, H. Takemoto, A. Ojida, K. Watanabe, A. Uemura, H. Kurose, T. Morii, T. Kobayashi, Y. Sato, C. Sato, I. Hamachi, Y. Mori, Selective and direct inhibition of TRPC3 channels underlies biological activities of a pyrazole compound, Proc. Natl. Acad. Sci. U.S.A. 106 (2009) 5400–5405.
[23] M.S. Kim, K.P. Lee, D. Yang, D.M. Shin, J. Abramowitz, S. Kiyonaka, L. Birnbaumer, Y. Mori, S. Muallem, Genetic and pharmacologic inhibition of the Ca(2+) influx channel TRPC3 protects secretory epithelia from Ca(2+)-dependent toxicity, Gastroenterology 140 (2011) 2107–2115.
[24] H.T. Ma, R.L. Patterson, D.B. van Rossum, L.B. aumer, K. Mikoshiba, D.L. Gill, Requirement of the inositol trisphosphate receptor for activation of store-operated Ca^{2+} channels, Science 287 (2000) 1647–1651.